Speckle Tracking Echocardiography Detects Uremic Cardiomyopathy Early and Predicts Cardiovascular Mortality in ESRD

Rafael Kramann,* Johanna Erpenbeck,* Rebekka K. Schneider,† Anna B. Röhl,‡ Marc Hein,‡ Vincent M. Brandenburg,§ Merel van Diepen,¶ Friedo Dekker,¶ Nicolaus Marx,§ Jürgen Floege,* Michael Becker,§ and Georg Schlieper*

*Division of Nephrology and Clinical Immunology, †Institute of Pathology, ‡Department of Anaesthesiology, and §Department of Cardiology, Medical Faculty RWTH Aachen University, Aachen, Germany; and ¶Department of Clinical Epidemiology, Leiden University Medical Center, Leiden, The Netherlands

ABSTRACT

Cardiovascular mortality is high in ESRD, partly driven by sudden cardiac death and recurrent heart failure due to uremic cardiomyopathy. We investigated whether speckle-tracking echocardiography is superior to routine echocardiography in early detection of uremic cardiomyopathy in animal models and whether it predicts cardiovascular mortality in patients undergoing dialysis. Using speckle-tracking echocardiography in two rat models of uremic cardiomyopathy soon (4–6 weeks) after induction of kidney disease, we observed that global radial and circumferential strain parameters decreased significantly in both models compared with controls, whereas standard echocardiographic readouts, including fractional shortening and cardiac output, remained unchanged. Furthermore, strain parameters showed better correlations with histologic hallmarks of uremic cardiomyopathy. We then assessed echocardiographic and clinical characteristics in 171 dialysis patients. During the 2.5-year follow-up period, ejection fraction and various strain parameters were significant risk factors for cardiovascular mortality (primary end point) in a multivariate Cox model (ejection fraction hazard ratio [HR], 0.97 [95% confidence interval (95% CI), 0.95 to 0.99; P=0.012]; peak global longitudinal strain HR, 1.17 [95% CI, 1.07 to 1.28; $P<0.001$]; peak systolic and late diastolic longitudinal strain rates HRs, 4.7 [95% CI, 1.23 to 17.64; P=0.023] and 0.25 [95% CI, 0.08 to 0.79; P=0.02], respectively). Multivariate Cox regression analysis revealed circumferential early diastolic strain rate, among others, as an independent risk factor for all-cause mortality (secondary end point; HR, 0.43; 95% CI, 0.25 to 0.74; P=0.002). Together, these data support speckle tracking as a postprocessing echocardiographic technique to detect uremic cardiomyopathy and predict cardiovascular mortality in ESRD.

J Am Soc Nephrol 25: 2351–2365, 2014. doi: 10.1681/ASN.2013070734

Patients with ESRD exhibit a dramatically increased risk for cardiovascular morbidity and mortality.[1–3] Interestingly, this fact is not mainly driven by the traditional atherosclerotic risk factors of the general population.[4] In contrast to the general population, where myocardial infarction and stroke are the predominant causes of cardiovascular death, sudden cardiac death (SCD) and recurrent heart failure are the most common causes of cardiovascular mortality in this patient group.[5–7] This might be caused by uremic cardiomyopathy (UC), a common complication in patients with ESRD that is characterized by cardiac fibrosis, capillary rarefaction, left ventricular hypertrophy, and both systolic and diastolic dysfunction.[8,9] In fact, two of

Received July 15, 2013. Accepted February 15, 2014.

M.B. and G.S. contributed equally to this work.

Published online ahead of print. Publication date available at www.jasn.org.

Correspondence: Dr. Rafael Kramann, Department of Nephrology and Clinical Immunology, Medical Faculty RWTH, Aachen University, Pauwelsstraße 30, 52074 Aachen, Germany. Email: rkramann@gmx.net

these characteristics—cardiac fibrosis and capillary rarefaction—trigger electric instability of the myocardium and thus may be directly related to SCD in patients with ESRD.[5] Therefore, early detection of UC in patients with ESRD might identify patients at risk for SCD and might have clinical impact on assessment and therapeutic decision-making in those patients.

Two-dimensional speckle-tracking echocardiography (STE) imaging is a relatively novel echocardiographic approach to assess regional left ventricular function by tracking acoustic markers (speckles) within the myocardium from frame to frame in B-mode images.[10,11] Many studies used this technique in comparison with conventional echocardiographic measures. Most conventional echocardiographic measures determine myocardial motion; the motion of any part of the myocardium is influenced by translational and tethering effects. STE analysis determines deformation and subtracts the effect of tethering and translational motion of the whole heart and is therefore superior to other echocardiographic measures regarding early changes of myocardial function. This was shown even in the setting of special patient cohorts.[12–15] Because it does not depend on the Doppler angle, as in tissue Doppler imaging, it allows assessment of strain and strain rate analyses in different myocardial axes (*i.e.*, longitudinal, circumferential, and radial). STE has been used to gain further insight into the pathophysiology of cardiac ischemia and infarction, and several primary diseases of the myocardium, such as hypertrophic or diabetic cardiomyopathy.[16–18] It has recently been appreciated that STE can also be used to identify areas of myocardial fibrosis,[19–24] one of the hallmarks of UC. This prompted us to evaluate in an animal study whether STE can detect early changes of left ventricular function and correlates with histologically determined severity of myocardial fibrosis in rat models of UC. Furthermore, in a clinical study we determined whether STE can predict cardiovascular and all-cause mortality in patients with ESRD.

RESULTS

Animal Study

Uremic Cardiomyopathy Was Characterized by Cardiac Hypertrophy and Interstitial Myocardial Fibrosis in Both Rat Models of CKD

To determine whether echocardiographically measured strain and strain rate values can detect early myocardial changes and myocardial fibrosis, we performed an animal study using STE combined with histological quantification of fibrosis in two rat models of CKD with uremic cardiomyopathy (*i.e.*, adenine-nephropathy and 5/6 nephrectomy; Figure 1). After induction of CKD, serum creatinine, urea, and phosphorus were significantly increased, whereas creatinine clearance was significantly decreased in both models of UC compared with the control group (Table 1). CKD was accompanied by significant myocardial hypertrophy (significantly increased cardiomyocyte cross-sectional area [Figure 2, A and B]) and increased heart weight (Figure 2C). Both heart weight and cardiomyocyte cross-sectional area showed a significant linear regression with serum phosphate (Figure 2, D and E). Quantitative real-time PCR of whole-heart mRNA expression revealed increased expression of β-myosin heavy chain and brain natriuretic peptide in both rat models of UC at the early and late time points (Figure 2, F and G).

Quantification of Masson trichrome–stained sections revealed a significant increase of interstitial extracellular matrix in both models of UC (Figure 3, A and B). The interstitial myocardial fibrosis was further characterized by increased expression of extracellular matrix proteins collagen 1α1, collagen 3α1, and fibronectin (Figure 3, C–F, Supplemental Figure 1) and upregulation of TGF-β mRNA transcripts (Figure 3G). Serum phosphate levels correlated significantly with the degree of interstitial myocardial fibrosis (Figure 3H).

STE Detected Early Impairment of Left Ventricular Systolic and Diastolic Deformation in Experimental Uremic Cardiomyopathy

Myocardial hypertrophy in both models of UC was confirmed by significantly increased thickness of the interventricular septum and the posterior wall as assessed by echocardiography (Table 2). Whereas standard echocardiographic measures, such as fractional shortening (FS), left ventricular stroke volume, and cardiac output (CO) were altered only at late time points (Figure 4, A and B, Table 2), left ventricular deformation parameters assessed by STE as peak global and systolic strain radial and circumferential (SR and SC peak G and peak S, respectively) were already significantly reduced at early time points (Figure 4, A and B, Table 2). Furthermore, strain rate parameters (*i.e.*, myocardial deformation per time unit) were significantly reduced at early and late time points in the radial orientation at both the systolic peak (SrR peak systolic) and the early diastolic peak (SrR diastolic peak E) (Figure 4, C and D). Thus, STE detected an early global (systolic and diastolic) impairment of left ventricular deformation in UC, which was not reflected in reduced conventional echocardiographic readouts of left ventricular function.

Myocardial Deformation Parameters Correlated Significantly with the Degree of Interstitial Myocardial Fibrosis and Myocardial Hypertrophy in Rats

We further asked whether the myocardial deformation parameters assessed by STE correlate with characteristics of UC. Several of the determined deformation parameters showed a higher correlation with the degree of interstitial fibrosis, the myocardial weight, and the cardiomyocyte cross-sectional area than the commonly used parameters of left ventricular function, such as FS or CO (Figure 5, Supplemental Table 1). Deformation parameters of the systolic and global left ventricular function as peak global radial and circumferential strain (Pearson correlation coefficient (PCC)=0.701 [$P<0.001$] and 0.678 [$P<0.001$], respectively), as well as the

Table 1. Humoral data from rats stratified for experimental groups and time points

Variable	Control Early	Adenine Nephropathy Early	5/6 Nephrectomy Early	Control Late	Adenine Nephropathy Late	5/6 Nephrectomy Late
S-creatinine[a] (μmol/L)	23±1.1	104±18.4[b,c]	72±19.8[b,c]	26±0.9	107±23.6[b]	86±17.8[b]
S-urea[a] (mmol/L)	6.4±0.4	13±1.2[b]	17.5±3[b]	6.9±0.6	17.5±3[b]	19±4.7[b]
S-phosphate[a] (mmol/L)	2.4±0.09	3.4±0.8[d]	3.8±0.47[e]	2.3±0.07	3.1±0.6[c,f]	4.2±0.9[b,c]
Creatinine clearance[g] (ml/min per kg)	8.9±0.44	3.5±0.68[b]	2.9±0.5[b]	8.7±0.52	2.7±0.31[b]	2.2±0.49[b]

Values are expressed as the mean±SD.
[a]Average over experiment, weekly determination.
[b]$P<0.001$ versus control.
[c]$P<0.05$ between adenine nephrectomy and 5/6 nephrectomy.
[d]$P<0.05$ versus control.
[e]$P<0.01$ versus control (one way ANOVA, *post hoc* Scheffe test).
[f]P=NS versus control.
[g]Average over experiment, determination every second week.

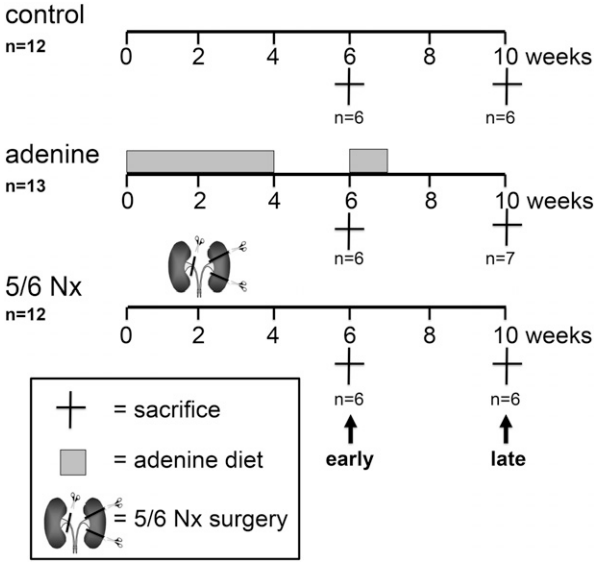

Figure 1. Experimental scheme of the animal study. High-phosphorus diet was given after subtotal nephrectomy (5/6 Nx).

peak systolic radial and circumferential strain rate (PCC=0.613 [$P<0.001$] and 0.611 [$P<0.001$], respectively), showed highly significant correlations with interstitial myocardial fibrosis (Figure 5, Supplemental Table 1). We additionally observed a significant correlation of these deformation parameters with factors of left ventricular hypertrophy as cardiomyocyte cross-sectional area and heart weight (Figure 5, Supplemental Table 1).

Importantly, the early diastolic peak SrR, as a diastolic left ventricular deformation parameter, also showed a close correlation with interstitial myocardial fibrosis (PCC=0.622; $P<0.001$) and with cardiomyocyte cross-sectional area and heart weight (PCC=0.7 [$P<0.001$] and 0.56 [$P<0.001$], respectively). This finding indicates that the systolic myocardial deformation intensity and the rate by which this deformation occurred during systole and diastole was significantly reduced in relation to increased cardiac hypertrophy and interstitial fibrosis.

Clinical Study

Patients

Of 985 patients with ESRD who underwent echocardiography in 2006, 2007, and 2008; 206 patients were identified as eligible with two-dimensional strain analysis accessible echocardiography. Thirty-five of these patients were excluded because of inappropriate image quality for strain analysis (Figure 6A). Thus, the study population comprised 171 patients with ESRD (111 men [64%]) undergoing dialysis (93% hemodialysis and 7% peritoneal dialysis; mean dialysis vintage±SD, 39±55 months; mean age, 64±14 years). Thirty-one of these patients had previously undergone kidney transplantation and had returned to dialysis 4.6±5.3 years before echocardiography.

Follow-Up

During the 2.1±0.9-year follow-up period, 42 patients (25%) reached the primary end point (cardiovascular mortality), on average after 311±302 days. The total mortality (secondary end point) during follow-up was 44% (*i.e.*, 75 patients died, after a mean of 302±285 days). In addition to the primary end point, causes of death were septicemia in 19 patients (11%), cancer in 7 (4%), and unknown in 7 (4%). Seventeen patients (10%) received a kidney transplant during follow-up, on average after 442±274 days. All 171 patients were included in the statistical analyses.

Baseline characteristics of survivors, nonsurvivors, and patients who reached the primary end point are outlined in Table 3. Compared with healthy persons (n=50), patients with ESRD showed a significant reduction of various left ventricular strain values (Supplemental Table 2).

In ESRD patients with diabetes mellitus (type 1 or 2), peak global longitudinal strain and early diastolic strain rate longitudinal were reduced by 10% and 17%, respectively, compared with ESRD patients without diabetes mellitus (−12.51±3.23 versus −11.26±3.3 [P=0.02] and 0.93±0.32 versus 0.77±0.32 [P=0.002], respectively) (Supplemental Table 3). Of note, less negative peak global longitudinal strain reflects reduced left ventricular deformation. We did not observe significantly altered strain parameters in hypertensive patients with ESRD compared with ESRD patients without hypertension (Supplemental Table 4).

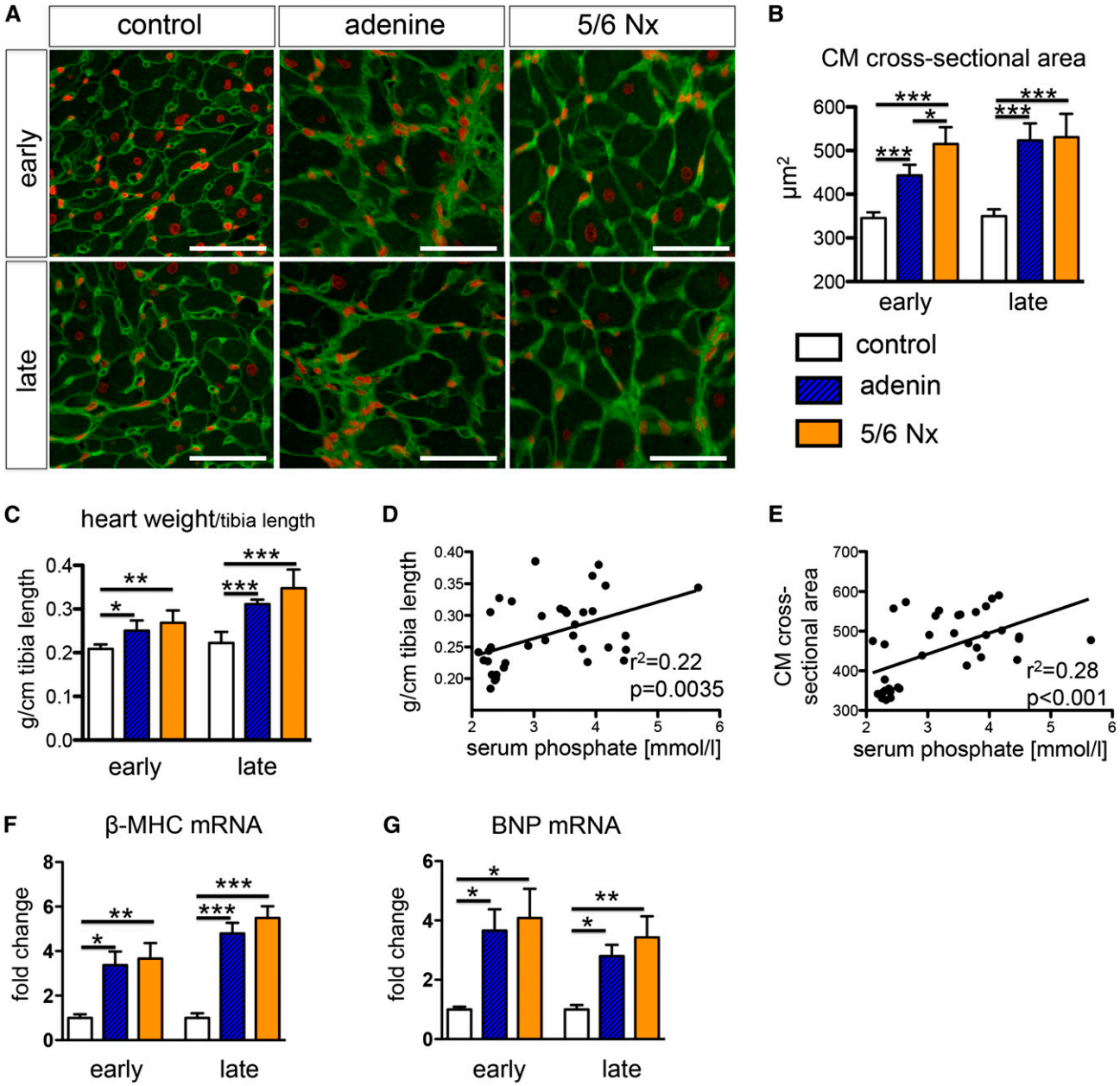

Figure 2. The severity of cardiac hypertrophy correlates with serum phosphate levels. (A and B) Wheat germ agglutinin (WGA) staining (A) and quantification of cardiomyocyte cross-sectional area (B) indicates hypertrophy of cardiomyocytes in both models of UC: early (*i.e.*, 4–6 weeks after induction of CKD) and late (8–10 weeks after induction of CKD). (C) Significantly increased heart weight in both models of UC at early and late time points. (D and E) Parameters of left ventricular hypertrophy show a significant linear regression with serum phosphate levels. (F and G) Quantitative real-time PCR analysis revealed significant cardiac upregulation of β-myosin heavy chain (MHC) (D) and brain natriuretic peptide (BNP) in both models of UC. *P<0.05; **P<0.01; ***P<0.001 (one-way ANOVA with *post hoc* Scheffe test). All scale bars=50 μm.

Strain longitudinal peak global was correlated with age (r=0.19; P=0.01); however, there was not a significant correlation with body mass index (r=0.13; P=0.11) (Supplemental Table 5).

Intra- and Interobserver Agreement

For intraobserver agreement, the Lin coefficient was 0.98 (95% confidence interval [95% CI], 0.97 to 0.99) for peak global longitudinal strain and 0.95 (95% CI, 0.90 to 0.990) for peak systolic longitudinal strain. For interobserver agreement, the Lin coefficient was 0.96 (95% CI, 0.94 to 0.98) and 0.90 (95% CI, 0.86 to 0.97), respectively. The Lin coefficients for the other strain parameters showed similar values.

Strain Parameters Predict Cardiovascular and All-Cause Mortality

In a Kaplan–Meier survival analysis, hemodialysis patients were categorized as being above (more negative) or below (less negative) the median (−11.83) of longitudinal peak

Table 2. Echocardiographic standard and speckle-tracking deformation parameters of rats stratified for experimental groups

Variable	Control Early	Adenine Nephropathy Early	5/6 Nephrectomy Early	Control Late	Adenine Nephropathy Late	5/6 Nephrectomy Late
Heart rate (beats/min)	306±32	314±31	309±18	310±23	308±28	307±18
LVIDs (cm)	0.33±0.08	0.4±0.09	0.37±0.08	0.35±0.05	0.42±0.04	0.48±0.08[a]
LVIDd (cm)	0.63±0.15	0.72±0.15	0.65±0.08	0.67±0.05	0.69±0.08	0.77±0.12
IVSs (cm)	0.18±0.03	0.28±0.04[a]	0.29±0.05[a]	0.19±0.02	0.35±0.13[b]	0.4±0.05[a]
IVSd (cm)	0.17±0.03	0.23±0.05[b]	0.26±0.05[a]	0.18±0.02	0.29±0.07[b]	0.32±0.05[a]
LVPWs (cm)	0.27±0.05	0.27±0.05	0.3±0.06	0.27±0.05	0.39±0.05[a]	0.38±0.04[a]
LVPWd (cm)	0.19±0.02	0.27±0.05[b]	0.28±0.04[a]	0.22±0.04	0.31±0.02[c]	0.31±0.02[c]
SV (ml)	0.26±0.04	0.26±0.02	0.24±0.02	0.26±0.01	0.23±0.03[b]	0.22±0.03[a]
SC peak G	−24±3.5	−18.5±1.8[b]	−18.4±2.6[b]	−22.9±3.4	−17±3.2[a]	−15.2±1.6[a]
SC peak S	−23.2±3.2	−17.6±1.6[b]	−16.4±3.8[b]	−21.1±3.4	−14±5.3[b]	−13.6±2[b]
SR peak G	30.5±5.9	16.8±3.3[c]	16.1±3.4[c]	29.9±6.3	12.8±4.2[c]	12.2±3.7[c]
SrC peak S	−6.2±0.8	−5.3±0.7	−4.7±0.2[a]	−6.1±1	−4.8±0.9	−4.1±1[a]
SrC peak E	6.2±0.56	6.2±1.1	4.7±2.3	6.4±1	4.1±2.3	3.9±2.3
SrR peak S	6.7±1.2	4.7±1[b]	4.6±1.5[b]	7.1±1.2	5±1.7[b]	4.7±0.6[b]
SrR peak E	−7±1.1	−5.2±0.9[b]	−3.8±1.3[c]	−7.3±0.8	−5.2±1.6[b]	−4.6±1.1[a]

Values are expressed as the mean±SD. LVIDs and LVIDd, left ventricular end-systolic and end-diastolic diameter; IVSs, septal thickness end-systolic; IVSd, septal thickness end-diastolic; LVPWs, left ventricular posterior wall thickness end-systolic; LVPWd, left ventricular posterior wall thickness end-diastolic; SV, stroke volume; SC peak G, strain circumferential global peak value; SC peak S, strain circumferential peak systolic value; SR peak G, strain radial peak global; SrC peak S, strain rate circumferential peak systolic value; SrC peak E, strain rate circumferential diastolic peak E; SrR peak S, strain rate radial systolic peak value; SrR peak E, strain rate radial diastolic peak E.

[a] $P<0.01$ versus control.

[b] $P<0.05$ versus control.

[c] $P<0.001$ versus control.

global strain. This analysis demonstrated that less negative longitudinal strain (peak global) was associated with an increased cardiovascular mortality (log-rank test: $P<0.001$) (Figure 6B).

Univariate Cox regression analysis revealed that apart from ejection fraction, several strain variables significantly differed between the patients who reached the primary or secondary endpoint and those who did not (Table 4).

Multivariate analysis (Table 5) for cardiovascular death or all-cause mortality did not change this observation. Various strain parameters were strong independent risk factors for cardiovascular and all-cause mortality (Table 5). Adding parameters such as protein, albumin, phosphate, potassium, C-reactive protein, or hemoglobin as potential confounders did not substantially change the results.

Crude effects of the clinical variables age, hypertension, diabetes, and body mass index, plus the parameters ejection fraction and longitudinal peak global strain, are shown in Supplemental Table 6. We included all these parameters in a multivariate analysis where only age and longitudinal peak global strain remained independent predictors of cardiovascular mortality (Supplemental Table 7).

DISCUSSION

Sudden cardiac death and chronic heart failure are the major causes of cardiovascular death in CKD and ESRD.[5–7] UC is the underlying pathophysiologic process and is characterized by myocardial hypertrophy and interstitial myocardial fibrosis.[9,25] Our study points toward a novel echocardiographic approach, STE, to detect UC and to predict cardiovascular and all-cause mortality in ESRD.

The pathogenesis of UC is incompletely understood. Increased levels of circulating factors, such as inflammatory cytokines, endogenous cardiotonic steroids, vasoactive hormones, and uremic toxins, might be involved.[26–31] Activation of the renin-angiotensin system is thought to be an important contributor to myocardial remodeling because in patients with ESRD, the severity of left ventricular hypertrophy correlates with plasma aldosterone concentration and administration of angiotensin-converting enzyme inhibitors improved structural changes as interstitial fibrosis in experimental and clinical studies.[32–34] Anemia, increased afterload due to aortic stiffness and hypertension, increased oxidative stress, and insulin resistance are other important contributors to the development of UC.[25,35,36] Another factor is hyperphosphatemia; in rats with subtotal nephrectomy, a high-phosphorus diet increased the severity of interstitial fibrosis and microvascular disease.[37] In patients free of known cardiovascular disease, dietary phosphorus was associated with a greater left ventricular mass.[38] The possible link between high phosphorus levels and cardiac hypertrophy might be increasing serum levels of fibroblast growth factor-23, which can induce left ventricular hypertrophy.[39]

We observed uremia with hyperphosphatemia and cardiac hypertrophy with interstitial fibrosis in both rat models of UC. The hyperphosphatemia was achieved by dietary phosphorus supplementation in the model of subtotal nephrectomy (5/6 nephrectomy), whereas the adenine nephropathy model is

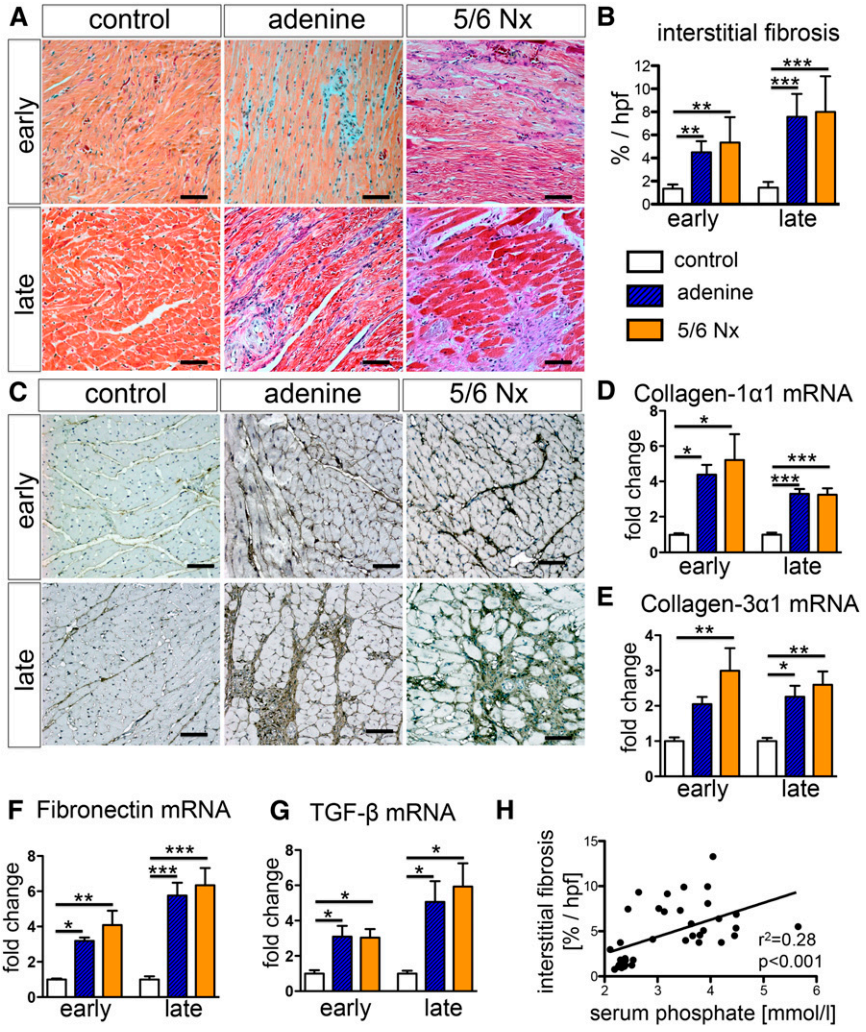

Figure 3. Uremic cardiomyopathy is characterized by interstitial myocardial fibrosis with upregulation of TGF-β expression. (A and B) Trichrome staining of hearts (A) and quantification (B) demonstrates significantly increased interstitial myocardial fibrosis in both models of UC at early and late time points. (C and D) Staining (C) and quantitative real-time PCR (D) for collagen 1α1 revealed increased expression in both rat models of UC. (E and F) Other extracellular matrix proteins, such as collagen 3α1 (E) and fibronectin (F), also showed increased expression of mRNA and protein levels (immunostaining: Supplemental Figure 1). (G) Quantitative real-time PCR showed increase expression of TGF-β mRNA transcript in both rat models of UC at early and late time points. (H) The severity of interstitial myocardial fibrosis did correlate significantly with serum phosphate levels. *P<0.05; **P<0.01; ***P<0.001 (one-way ANOVA with *post hoc* Scheffe test). All scale bars=50 μm.

known for its severe hyperparathyroidism.[40,41] Serum phosphate levels correlated significantly with the grade of cardiac hypertrophy as heart weight and cardiomyocyte cross-sectional area and the severity of myocardial fibrosis.

TGF-β is a known key player in solid organ fibrosis[42] and has been implicated in the development of UC.[31,43] We observed a significant upregulation of TGF-β in both rat models of UC. Additionally, UC was accompanied by re-expression of the fetally expressed β-myosin heavy chain and increased cardiac expression of brain natriuretic peptide, both of which have been linked to cardiac fibrosis, hypertrophy, and UC.[31,44,45]

Our first major finding was that, in rat models, UC led to early changes of myocardial systolic and diastolic deformation detectable by STE, whereas classic echocardiographic parameters of left ventricular function, such as FS or CO, changed only at a later time point, when the rats exhibited greater myocardial fibrosis and hypertrophy. Martin *et al.* recently reported early changes in early diastolic circumferential strain rate assessed by STE in rats with mild renal insufficiency after uninephrectomy.[43] This is in line with our finding of early changes in peak diastolic strain rate, but we observed predominant changes in peak global and systolic strain in our rat models of UC. This discrepancy might be explained by our more severe model of UC with more advanced CKD and higher degrees of interstitial fibrosis resulting in a left ventricular systolic impairment in addition to the reduced diastolic deformation.

Our second important finding was that speckle-tracking parameters correlated significantly with the grade of myocardial fibrosis and hypertrophy in both rat models of UC.

In line with our results, Pen *et al.* described a significant correlation of both radial and circumferential strain to interstitial myocardial fibrosis and myocyte cross-sectional area in mouse models of cardiac dysfunction (transverse aortic constriction and profound isoflurane anesthesia).[24] However, these authors observed a higher correlation for circumferential strain with interstitial fibrosis than for radial strain.[24] In a rat model of doxorubicin cardiomyopathy, Migrino *et al.* observed an early reduction of radial strain after 8 weeks; the fractional shortening changed later, after 12 weeks.[46] The correlation of global and systolic strain and strain rate parameters with the severity of cardiac fibrosis might be explained by the fact that fibrosis represents a loss of functional cardiomyocytes that are replaced with scar tissue, resulting in impaired systolic left ventricular deformation.[24] Moreover, interstitial myocardial fibrosis might lead to increased left ventricular stiffness, thereby explaining the correlation with diastolic strain parameters in particular early diastolic strain rate radial. Early diastolic strain rate has the advantage of reflecting the diastolic performance of all myocardial segments by a

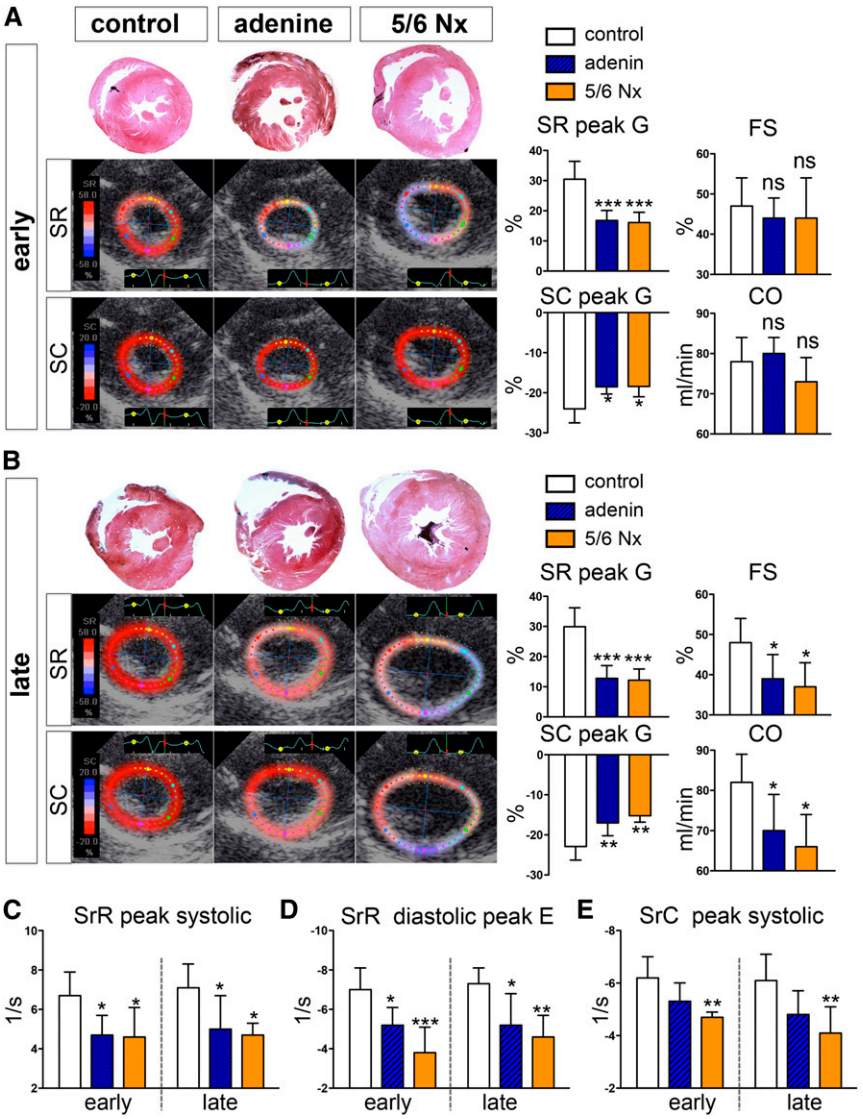

Figure 4. Uremic cardiomyopathy leads to early impairment of left ventricular systolic and diastolic deformation. (A) At the early time points (*i.e.*, 4–6 weeks after induction of CKD), both peak global radial and circumferential strain (SR peak G, SC peak G) were already significantly reduced, whereas standard-echocardiographic parameters, such as FS and Duplex ultrasonographically determined CO, remained unchanged. Representative parasternal short-axis views with color-coded radial and circumferential strain show a dramatic reduction in predominantly radial strain. (B) At late time points (8–10 weeks after induction of CKD), in addition to the myocardial deformation parameters (SR peak G and SC peak G), conventional echocardiographic readouts of left ventricular function FS and CO show a significant decrease. (C–E) Strain rate parameters indicating the rate by which the myocardial deformation occurs (deformation/time unit) were significantly reduced at early and late time points in the radial orientation at both the systolic peak (SrR peak systolic [C]) and the early diastolic peak (SrR diastolic peak E [E]) in both rat models of UC. In contrast, the peak systolic rate of myocardial deformation in the circumferential direction (SrC peak systolic) was significantly reduced only in the 5/6 nephrectomy (Nx) model of UC. *$P<0.05$; **$P<0.01$; ***$P<0.001$ versus control group.

regional measurement.[47] Recently, a significant correlation between left ventricular filling pressure and early diastolic strain rate was shown.[48] Thus, this parameter may describe a sensitive and physiologic approach to integrating myocardial relaxation characteristics and hemodynamics. Furthermore, researchers reported that early diastolic strain rate is superior to tissue Doppler imaging–derived analysis and is independently associated with the outcome in acute myocardial infarction.[47] In line with this, we found that early diastolic strain rate is an independent risk factor for all-cause mortality in patients with ESRD. Interestingly, this parameter is impaired in segments at risk despite near-normal systolic deformation.[49]

Late gadolinium enhancement imaging *via* cardiac magnetic resonance imaging is the gold standard method for the noninvasive evaluation of cardiac fibrosis.[50] Fibrosis severity detected *via* late gadolinium enhancement correlates significantly with STE-assessed strain parameters in patients with hypertrophic cardiomyopathy and Fabry disease.[19,20,23] However, in patients with higher-stage CKD and those with ESRD, gadolinium is contraindicated because of the risk of nephrogenic systemic fibrosis.[51] The earlier detection of myocardial fibrosis in UC using STE compared with standard echocardiographic readouts can thus possibly be used for interventional trials in patients with CKD and ESRD.

Our third major finding was that speckle-tracking parameters, such as peak global longitudinal strain, peak systolic longitudinal strain rate, and peak global circumferential and radial strain, were independent risk factors for cardiovascular mortality. In 201 patients with heart failure (number of patients with CKD not stated), Cho *et al.* reported that global circumferential strain is an independent and better predictor of cardiac events (readmission for heart failure or cardiac death) than left ventricular ejection fraction.[52]

Several studies described a reduction of left ventricular strain parameters in patients with CKD or ESRD despite preserved left ventricular ejection fraction.[53–55] Edwards *et al.* reported that patients with early-stage CKD (CKD stages 2–3) have impaired systolic strain and strain rate values (assessed by

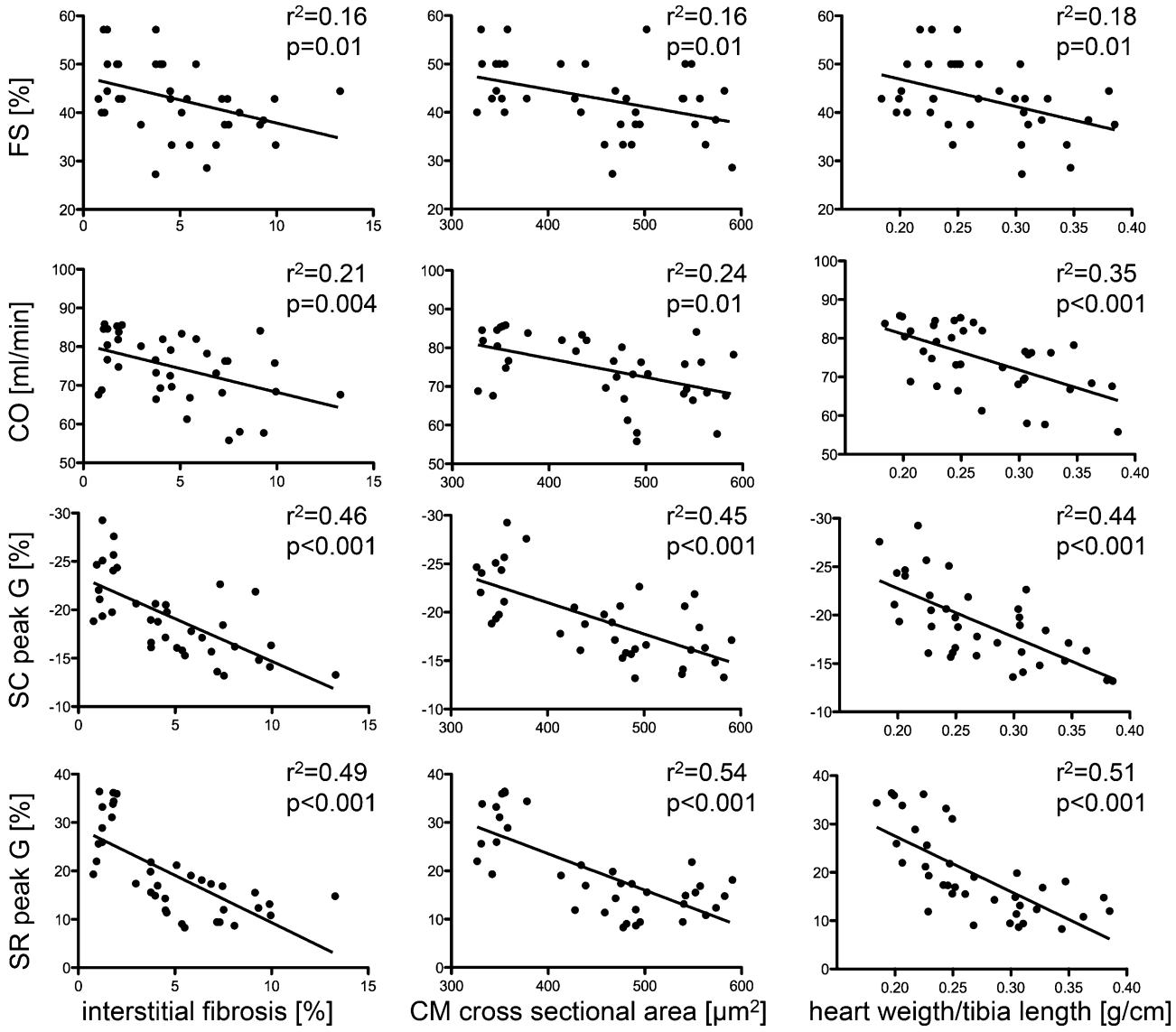

Figure 5. Global circumferential and radial strain and hallmarks of UC are significantly correlated. Speckle-tracking parameters correlate highly significant with hallmarks of UC, such as interstitial fibrosis, myocardial weight, and cross-sectional cardiomyocyte diameter. CM, cardiomyocyte; SC peak G, strain circumferential peak global; SR peak G, strain radial peak global.

tissue Doppler imaging), whereas the conventional echocardiographic parameters of left ventricular function as ejection fraction remain unchanged compared with healthy persons without CKD.[56] Rahkit *et al.* used tissue Doppler imaging in patients with CKD and did show that diastolic tissue velocity is an independent predictor of cardiovascular events.[57] Recently, Liu *et al.* reported that global longitudinal strain is an independent predictor of all-cause mortality in patients with ESRD who have preserved left ventricular function.[58] Although radial, circumferential, and longitudinal fibers are predominantly in different layers of the myocardium, we observed reduced myocardial deformation in all these orientations when we compared our ESRD patient cohort to healthy persons. As heart muscle is incompressible, strain parameters are interrelated in three dimensions; thus, by the time the chamber contracts and shortens in systole (circumferential and longitudinal strain), the wall thickens (radial strain).[59]

As a postprocessing computer algorithm of routine gray-scale images, speckle-tracking analysis can easily been integrated into clinical standard procedures and may help to detect UC and define patients with ESRD at high risk for cardiovascular death. An early detection of UC might be the basis for interventional trials and could help to initiate secondary prevention strategies, such as improved chronic heart failure therapy and implantation of cardioverter-defibrillators, which might lead to a reduction of cardiovascular mortality in ESRD. In fact, the current rates of implantable cardioverter-defibrillators in patients with ESRD are very low despite these

Table 3. Baseline demographic and clinical characteristics stratified for survivors, nonsurvivors, and patients who died of cardiovascular disease during follow-up

Characteristic	Survivors (*n*=96)	Nonsurvivors (*n*=75)	*P* Value[a]	CV Death (*n*=42)	*P* Value[a]
Age (yr)	61±14	69±11	<0.001	70±11	<0.001
Men, *n* (%)	59 (61)	52 (69)	0.33	30 (71)	0.34
Body mass index (kg/m^2)	27±5	26±6	0.64	27±6	0.96
BP systolic/diastolic (mmHg)	131±20/73±13	134±16/71±11	0.45/0.39	132±17/69±7	0.9/0.1
Smokers, *n* (%)	21 (22)	22 (29)	0.49	12 (29)	0.73
Previous diagnoses, *n* (%)					
Hypertension	69 (72)	55 (73)	0.86	31 (74)	1
Coronary artery disease	50 (52)	52 (69)	0.03	33 (79)	0.004
STEMI	11 (11)	12 (16)	0.5	8 (19)	0.29
NSTEMI	27 (28)	28 (37)	0.25	17 (40)	0.17
Coronary stent	15 (16)	18 (24)	0.18	13 (31)	0.06
Coronary artery bypass	14(15)	12 (16)	0.83	7 (17)	0.8
Peripheral artery occlusive disease	13 (14)	25 (33)	0.003	19 (45)	<0.001
Prior stroke	21 (22)	17 (23)	1.0	12 (29)	0.52
Valvular heart disease	38 (40)	36 (48)	0.28	19 (45)	0.58
Congestive heart failure	19 (20)	22 (29)	0.15	15 (36)	0.06
Atrial fibrillation	26 (27)	40 (53)	<0.001	24 (57)	<0.001
Pacemaker	7 (7)	8 (11)	0.59	5 (12)	0.51
Biventricular pacemaker	0	2 (3)	0.20	2 (5)	0.09
Dilative cardiomyopathy	4(4)	5 (7)	0.51	3 (7)	0.68
Ischemic cardiomyopathy	5(5)	4 (5)	1.0	2 (5)	1
Diabetes mellitus type 1 or 2	37 (39)	28 (37)	1.0	22 (52)	0.45
Secondary hyperparathyroidism	55(57)	39 (52)	0.54	21 (50)	0.46
Cause of ESRD, *n* (%)					
Diabetic nephropathy	25 (26)	24 (32)	0.40	16 (40)	0.15
Nephrosclerosis	26 (27)	20 (27)	1.0	12 (29)	1
Chronic GN	18 (19)	13 (17)	0.84	6 (14)	0.63
Polycystic kidney disease	15 (16)	3 (4)	0.01	1 (2)	0.02
Interstitial nephritis	4 (4)	5 (7)	0.51	0	0.3
Systemic disease[b]	4 (4)	3 (4)	1.0	3 (7)	0.68
Unknown	4 (4)	7 (9)	0.22	4 (10)	0.25
Medications, *n* (%)					
β-Blocker	79 (82)	53 (71)	0.1	30 (17)	0.18
ACE inhibitor	47(49)	27 (36)	0.12	18 (43)	0.58
Angiotensin II–receptor antagonist	19 (20)	12 (16)	0.55	10 (24)	0.65
Calcium channel blocker	42 (44)	28 (37)	0.44	15 (36)	0.46
Diuretic	61 (64)	41 (55)	0.27	25 (60)	0.7
Sympatholytics[c]	23 (24)	11 (15)	0.18	6 (14)	0.26
Statin	38 (40)	34 (45)	0.53	20 (48)	0.35
Amiodarone	7 (7)	4 (5)	0.76	2 (5)	0.72
Phosphate binder					
Calcium-containing	50 (52)	37 (49)	0.76	20 (48)	0.71
Non–calcium-containing	35 (36)	21 (28)	0.26	11 (26)	0.25
Cinacalcet	9 (9)	3 (4)	0.23	2 (5)	0.5
Vitamin D	53 (55)	35 (47)	0.28	21 (50)	0.58
Erythropoietin	55 (57)	39 (52)	0.54	15 (36)	0.03
Phenprocoumon	19 (20)	16 (21)	0.85	11 (26)	0.5
Dialysis-related informations					
Time on dialysis (mo)	43±66	33±45	0.21	33±46	0.31
Duration of dialysis (hr/wk)	12±3	12±3	0.91	12±3	0.68
Frequency of dialysis (d/wk)	3±0.6	3±0.9	0.49	3±1.2	0.68
Ultrafiltration volume (ml)	2065±1247	2179±1779	0.71	2383±2245	0.52
Peritoneal dialysis, *n* (%)	6 (6)	2 (3)	0.47	0	0.18
Arteriovenous fistula, *n* (%)	65 (68)	37 (49)	0.02	25 (60)	0.44

Table 3. Continued

Characteristic	Survivors (*n*=96)	Nonsurvivors (*n*=75)	*P* Value[a]	CV Death (*n*=42)	*P* Value[a]
Central catheter, *n* (%)	30 (31)	38 (51)	0.01	17 (40)	0.33
Laboratory values					
Potassium (mmol/L)	4.7±0.8	4.6±0.8	0.54	4.7±0.8	0.98
Calcium (mmol/L)	2.24±0.3	2.19±0.3	0.22	2.21±0.22	0.54
Phosphorus (mmol/L)	1.7±0.7	1.64±0.6	0.58	1.55±0.53	0.25
Protein (g/L)	68±8	65±9	0.01	67±8	0.39
Albumin (%)	55±11	48±10	0.005	48±9	<0.01
Hemoglobin (g/L)	112±16	107±17	0.05	109±18	0.43
Parathyroid hormone (ng/L)	290±300	201±217	0.10	175±192	0.06

Values expressed with a plus/minus sign are the mean±SD. STEMI, ST-segment elevation myocardial infarction; NSTEMI, non–ST-segment elevation myocardial infarction; ACE, angiotensin-converting enzyme.
[a]Versus survivors; Fisher exact test.
[b]Lupus erythematosus, sarcoidosis, rheumatoid arthritis, Wegener granulomatosis, Henoch-Schönlein purpura, Churg-Strauss arteritis, polyarteritis nodosa.
[c]Clonidine or moxonidine.

Table 4. Univariate Cox analysis

Parameter	Total Mortality		Cardiovascular Mortality	
	HR (95% CI)	*P* Value	HR (95% CI)	*P* Value
EF	0.98 (0.97 to 0.99)	0.04	0.98 (0.96 to 0.99)	0.01
SL peak G	1.13 (1.06 to 1.21)	<0.0001	1.23 (1.13 to 1.35)	<0.001
SL peak S	1.12 (1.05 to 1.19)	0.001	1.21 (1.10 to 1.32)	<0.001
SrL peak S	1.99 (0.81 to 4.85)	0.13	8.82 (2.41 to 32.21)	<0.001
SrL peak E	0.90 (0.44 to 1.82)	0.77	0.39 (0.16 to 0.98)	0.045
SrL peak A	1.16 (0.93 to 1.45)	0.20	0.16 (0.05 to 0.51)	0.002
SC peak G	1.10 (1.05 to 1.15)	<0.001	1.09 (1.02 to 1.15)	<0.01
SC peak S	1.1 (1.05 to 1.15)	<0.001	1.09 (1.03 to 1.16)	<0.01
SrC peak S	1.71 (0.96 to 3.04)	0.07	1.73 (0.78 to 3.82)	0.18
SrC peak E	0.41 (0.24 to 0.68)	0.001	0.53 (0.26 to 1.06)	0.07
SrC peak A	0.83 (0.53 to 1.30)	0.42	0.80 (0.42 to 1.51)	0.49
SR peak G	0.97 (0.96 to 0.99)	0.003	0.97 (0.95 to 0.99)	0.01
SrR peak S	0.62 (0.40 to 0.94)	0.03	0.59 (0.33 to 1.06)	0.08
SrR peak E	1.53 (1.09 to 2.17)	0.02	1.31 (0.82 to 2.10)	0.25
SrR peak A	1.37 (0.96 to 1.94)	0.08	1.13 (0.71 to 1.79)	0.61

For all strain parameters with a negative sign (*i.e.*, SL peak G, SL peak S, SrL peak S, SC peak G, SC peak S, SrC peak S, SrR peak E, and SrR peak A), the hazard ratio is >1 because a higher value for these parameters indicates less myocardial contraction (strain) or contraction velocity (strain rate).
HR, hazard ratio; EF, ejection fraction; SL peak G, strain longitudinal peak global value; SL peak S, strain longitudinal peak systolic; SrL peak S, strain rate longitudinal peak systolic; SrL peak E, strain rate longitudinal diastolic peak E; SrL peak A, strain rate longitudinal diastolic peak A; SC peak G, strain circumferential global peak value; SC peak S, strain circumferential peak systolic value; SrC peak S, strain rate circumferential peak systolic value; SrC peak E, strain rate circumferential diastolic peak E; SrC peak A, strain rate circumferential diastolic peak A; SR peak G, strain radial peak global value; SrR peak S, strain rate radial systolic peak value; SrR peak E, strain rate radial diastolic peak E; SrR peak A, strain rate radial diastolic peak A.

patients' high risk for SCD[60]; thus, new strategies for risk assessment are urgently needed.

The study had some limitations. The radial and circumferential strain and strain rate values in this study reflect the myocardial contractility in the six midventricular segments because we determined strain values only from midventricular short-axis views in both rats and humans. Thus, we cannot exclude the possibility that the strain and strain rate parameters of the whole left ventricle, including the apex and basal levels, would be different. Because left ventricular contractility may differ between rats and humans,[61] we cannot entirely extrapolate our observed animal echocardiography data to dialysis patients.

In conclusion, STE detects early interstitial fibrosis and changes in left ventricular contractility in rat models of UC and predicts cardiovascular and all-cause mortality in patients with ESRD.

CONCISE METHODS

Animal Study

Local government authorities approved all animal experiments reported in this article, and all animal experiments adhered to the National Institutes of Health's Guide for the Care and Use of Laboratory Animals. A total of 37 male Wistar rats (Charles River Laboratories, Borken, Germany) weighing 290–320 g were studied. We used two different models of UC:

1. We performed 5/6 nephrectomy in a one-step surgery: Rats were anesthetized (xylazine/ketamine intraperitoneal), and a 6-cm incision was made in the linea alba; the right kidney was exposed, unencapsulated, and removed after ligation of its pedicle. Thereafter, the left kidney artery was exposed. Two of the normally three segment arteries were ligated (7-0 suture; Monofil, Ethicon) after visualization of the renal perfusion of these arteries *via* short forceps clamping/unclamping to make sure that only one third of the kidney remains perfused. To aggravate the myocardial fibrosis, rats were fed a high-phosphorus (1.2%) diet (Altromin, Lage, Germany).

2. Adenine nephropathy was induced by feeding rats a diet containing 0.75% adenine and 2.5% protein (Altromin) over 4 weeks, as described previously.[62] Because decrease in renal function in the

Table 5. Multivariate Cox analysis

Parameter	Total Mortality		Cardiovascular Mortality	
	HR (95% CI)	*P* Value	HR (95% CI)	*P* Value
EF	0.98 (0.97 to 0.99)	<0.05	0.97 (0.95 to 0.99)	0.012
SL peak G	1.10 (1.03 to 1.17)	<0.01	1.17 (1.07 to 1.28)	<0.001
SL peak S	1.10 (1.03 to 1.17)	<0.01	1.17 (1.07 to 1.28)	<0.001
SrL peak S	1.27 (0.53 to 3.03)	1.0	4.66 (1.23 to 17.64)	0.023
SrL peak A	1.25 (0.99 to 1.57)	0.06	0.25 (0.08 to 0.79)	<0.02
SC peak G	1.09 (1.04 to 1.14)	<0.001	1.08 (1.01 to 1.14)	<0.02
SC peak S	1.09 (1.04 to 1.14)	<0.001	1.08 (1.02 to 1.15)	0.01
SC peak P	1.12 (1.00 to 1.24)	0.04	1.14 (0.96 to 1.34)	0.13
SrC peak E	0.43 (0.25 to 0.74)	0.002	0.69 (0.34 to 1.40)	0.30
SR peak G	0.98 (0.96 to 0.99)	<0.01	0.97 (0.95 to 1.00)	0.03
SrR peak E	1.45 (1.01 to 2.09)	<0.05	1.16 (0.70 to 1.92)	0.6

The multivariable-adjusted Cox regression analysis accounted for age, sex, diabetes, and presence of cardiovascular disease at the start of the study as possible confounders (*i.e.*, known coronary artery disease, coronary stent, prior ST-segment elevation myocardial infarction or non–ST-segment elevation myocardial infarction, prior stroke, ischemic cardiomyopathy). Note that only the significant data are presented. HR, hazard ratio; EF, ejection fraction; SL peak G, strain longitudinal peak global value; SL peak S, strain longitudinal peak systolic; SrL peak S, strain rate longitudinal peak systolic; SrL peak A, strain rate longitudinal diastolic peak A; SC peak G, strain circumferential global peak value; SC peak S, strain circumferential global peak systolic; SC peak P, strain circumferential peak positive; SrC peak E, strain rate circumferential diastolic peak E; SR peak G, strain radial peak global value; SrR peak E, strain rate radial diastolic peak E.

adenine model takes about 2 weeks to reach a level of CKD similar to that in the 5/6 nephrectomy model directly after surgery, we compared rats in the adenine nephropathy model 6 and 10 weeks after start of the diet with the 5/6 nephrectomy rats 4 and 8 weeks after surgery, respectively (Figure 1). The 10-week adenine group was fed an additional week of the adenine diet after 6 weeks.

Echocardiography was performed at 6 and 10 weeks (*i.e.*, 4 and 8 weeks after 5/6 nephrectomy surgery) (Figure 1). Serum samples were collected weekly from the tail vein. After echocardiography the rats were euthanized by exsanguination.

Echocardiography and Two-Dimensional Strain Analysis in Rats

After rats were anesthetized (80 mg/kg ketamine delivered intraperitoneally) and shaved, echocardiographic data were acquired using a Vivid I echocardiography machine (GE Healthcare, Horton, Norway) and an 11.5-MHz 10S-RS sector transducer. Image depth was 2–2.5 cm, and the frame rate was 190–225 frames per second. Images were stored and analyzed offline using EchoPAC-PC software (GE Healthcare). Left ventricular size and systolic and diastolic diameter of the interventricular and the posterior wall were measured using M-Mode in the parasternal short axis view at the level of the papillary muscles. FS was calculated as follows:

$$FS = (LVIDd - LVIDs)/LVIDd \times 100\%.$$

Aortic annulus diameter was measured during systole from two-dimensional images. Diameter of pulmonary annulus and velocity time integral of continuous wave Doppler images were obtained from the short-axis view. Stroke volume was estimated as described previously.[63] CO was calculated by multiplication of stroke volume with heart rate.

Speckle tracking analysis was performed using the Q-analysis software within EchoPAC-PC software (GE Healthcare) as described previously.[64] Left ventricular radial and circumferential peak systolic strain and strain rate were assessed in the midventricular parasternal short axis view using papillary muscles as landmarks.

Quantitative Real-Time PCR

Quantitative real-time PCR was carried out as previously described.[65] TaqMan primers and probes were designed from sequences in the GenBank database using the Primer Express software (Applied Biosystems, Foster City, CA). Primers are listed in Supplemental Table 8.

Miscellaneous Measurements

Serum and urine biochemistries were performed by standard laboratory procedures using an automated analyzer.

Histomorphological Analysis

For histologic and immunohistochemical analyses, tissue sections were fixed in 3.7% formaldehyde for 24 hours, paraffin embedded, cut with a rotating microtome at 3-μm thickness (Leica Microsystems), and stained according to routine histology protocols. Immunohistochemical analysis was performed using primary antibodies specific for fibronectin (rabbit polyclonal, 1:50; EMD Millipore, Billerica, MA), collagen I and III (both goat polyclonal, 1:100; Southern Biotec, Birmingham, AL). Antigen demarcation was achieved by microwave pretreatment in citrate buffer (pH, 6.0). After blocking (Blocking Kit; Vector Laboratories, Burlingame, CA) and 3% H_2O_2 treatment, sections were incubated with the primary antibody. Biotinylated horse monoclonal anti-goat and horse monoclonal anti-rabbit antibody (Vector Laboratories) were used as secondary antibodies. Detection was realized using the Vectastin ABC Kit (Vector Laboratories). Slides were counterstained with hematoxylin.

Histologic Measurements

To visualize cardiomyocyte borders, fixed tissue was incubated in wheat germ agglutinin conjugated to Alexa Fluor 488 (Invitrogen) at 1 mg/ml in PBS containing 10 mM sodium azide. ImageJ software (National Institutes of Health, Bethesda, MD) was used to quantify cross-sectional cell surface area of 30 cells per field in each of four different myocardial regions (lateral, anterior, septal, and posterior) in a short-axis midventricular section. Quantification of myocardial fibrosis in Masson trichrome–stained sections, collagen I and III– and fibronectin-positive surface area, were determined in midventricular short-axis sections at 200× magnification (10 pictures per rat) using the number of stained pixels per total pixels in Adobe Photoshop CS5 (Adobe Systems, Inc., San Jose, CA).

Clinical Study

Patients

Patients with ESRD (undergoing hemodialysis or peritoneal dialysis treatment with a mean dialysis vintage of 38 months [determinable in 153 of 171 patients]) who had echocardiography in the RWTH Aachen University Hospital Department of Cardiology between January 1,

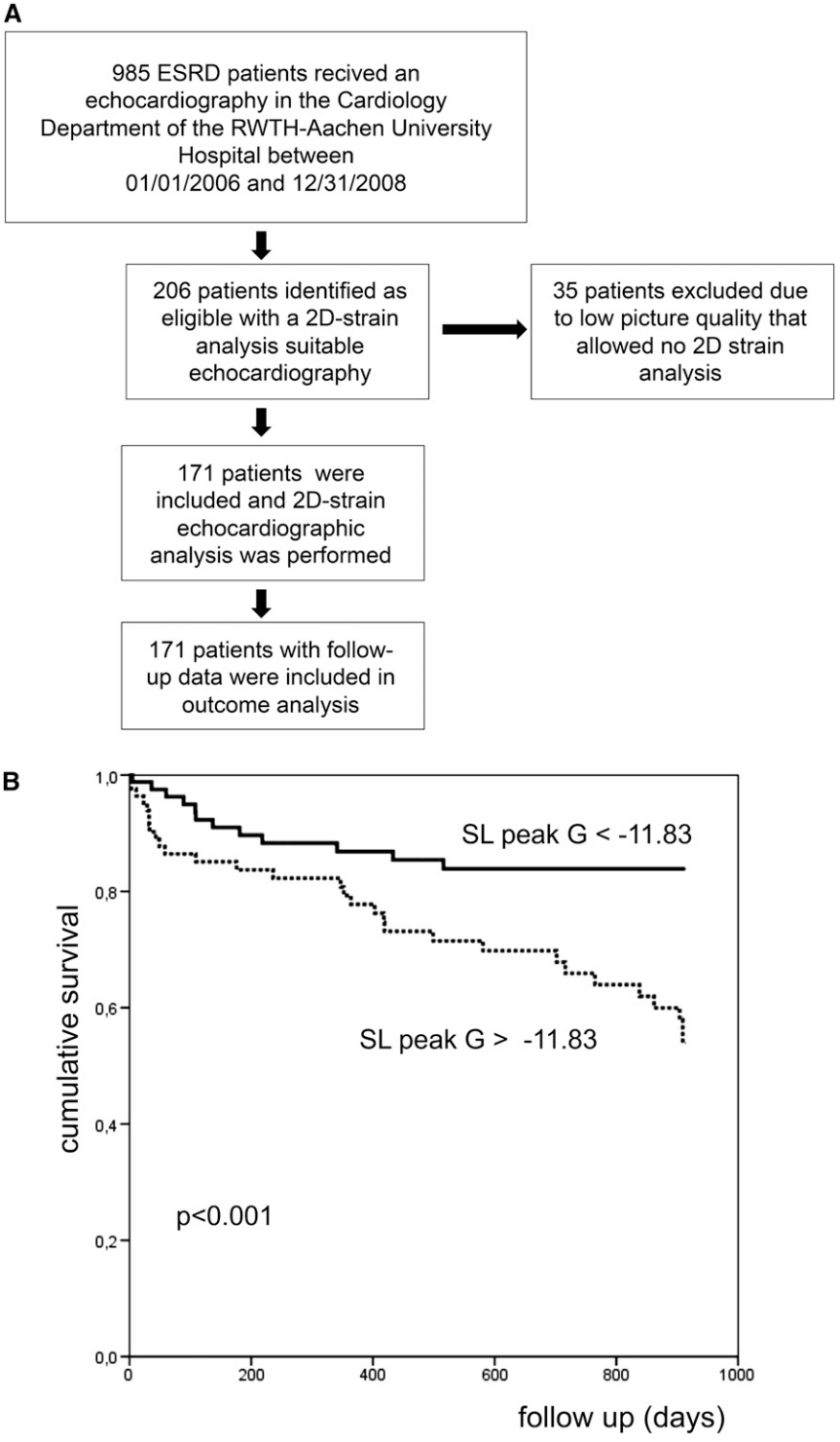

Figure 6. Less negative strain longitudinal peak global is associated with a higher cardiovascular mortality in patients with ESRD. (A) Flow chart of the clinical study. (B) Kaplan–Meier analysis of cumulative cardiovascular survival for patients with a peak global longitudinal strain stratified at the median (−11.83), indicating that a less negative peak global longitudinal strain (lower myocardial deformation) was associated with a higher cardiovascular mortality (primary end point). Statistical comparisons between survival curves were made by log-rank test. 2D, two-dimensional; SL peak G, strain longitudinal peak global.

2006, and December 31, 2008, were screened for study eligibility. Patients with echocardiography that was no suitable for speckle-tracking analysis (*i.e.*, echocardiography was not performed on the adequate machine or picture quality was too low for strain analysis) were excluded. Additionally, to compare the echocardiographic speckle-tracking values of patients with ESRD with strain values of healthy persons, we included 50 age-matched participants (31 men [62%]); mean age, 63±12 years; serum creatinine level <106 μmol/L) who had a normal left ventricular ejection fraction (>55%, biplane Simpson method) and, apart from a small percentage with hypertension (20%), were free of any known cardiovascular disease or other cardiovascular risk factors.

The study was approved by the ethical committee of the RWTH Aachen University Hospital (EK167/11) and carried out according to the Declaration of Helsinki. Follow-up data were obtained from patients with ESRD. Data on medical history, medications, and biochemical data were obtained by retrospective chart review.

Two-Dimensional Echocardiography and Speckle Tracking Analysis

The present study is based on echocardiographic two-dimensional loops that were all prospectively recorded in the echocardiography unit of the Cardiology Department in our hospital using a digital ultrasound scanner (Vivid 7; GE Healthcare) equipped with a 2.5-MHz transducer. Left ventricular apical two-, three-, and four-chamber views and left ventricular parasternal short-axis view at midventricle were acquired and processed. Left ventricular ejection fraction was measured offline on a personal computer with EchoPAC-PC software (version 110.1.3; GE Healthcare) by manual tracing of end-systolic and end-diastolic endocardial borders in apical two- and four-chamber views, applying the Simpson biplane method. The frame rate for the investigations was between 50 and 90 frames per second.

Speckle-tracking analysis was performed retrospectively and offline with the above-mentioned software package; we used the first cardiac cycle of each acquired loop as described elsewhere.[16,66] Peak systolic and global longitudinal strain and peak systolic and diastolic longitudinal strain rate were obtained for each segment in an 18-segment left ventricular model (6 segments at each apical view). Peak systolic and global circumferential and radial strain and peak systolic and

diastolic circumferential and radial strain rates were assessed in 6 segments of the parasternal short-axis view at the mid-ventricular level. The software package automatically grades the tracking quality of each segment on a scale ranging from 1.0 (optimal) to 3.0 (inadequate). Only segments with a tracking quality of ≤2.0 were included in the analysis. The investigator was blinded to the patients' outcome data. All hemodialysis patients underwent echocardiography on a nondialysis day.

Outcomes

Cardiovascular death was defined as the primary end point. Death by any cause was the secondary end point. Follow-up was performed by review of the patients' hospital chart or telephone interview with the patient or the patient's primary healthcare providers and through the government death registry. Death occurring outside the hospital for which no other cause was specified was regarded as SCD and was included in the definition of cardiovascular death if the patient had known cardiovascular disease (*i.e.*, prior myocardial infarction or chronic heart failure) and was not diagnosed with cancer.

Statistical Analyses

All analyses were done using SPSS software, version 18 (SPSS, Inc., Chicago, IL) using Windows 7. Continuous factors were summarized by means±SDs. Categorical data were presented by relative frequencies and percentages. A *t* test was used to compare differences between two groups for continuous variables, and the Fisher exact test was used to compare differences between two groups for categorical variables.

The Kaplan–Meier method was used to estimate cumulative survival. To identify the prognostic factors of all-cause and cardiovascular death, comparisons between survival curves were made by log-rank test. Cox regression was used (the "enter" method) to determine the effect of strain parameters on all-cause and cardiovascular mortality. The multivariable adjusted Cox regression analysis accounted for age, sex, diabetes, and presence of cardiovascular disease at the start of the study as possible confounders (*i.e.*, known coronary artery disease, coronary stent, prior ST-segment elevation myocardial infarction or non–ST-segment elevation myocardial infarction, prior stroke, ischemic cardiomyopathy).

All test results are reported as hazard ratios, corresponding 95% CIs, and *P* values. In the animal study, for multiple group comparison, ANOVA with *post hoc* Scheffe correction was applied. Analyses were performed using the above-mentioned SPSS software or GraphPad Prism (5.0c, GraphPad Software, Inc., La Jolla, CA). Statistical significance was defined as $P<0.05$.

To define interobserver and intraobserver variability in analysis of myocardial deformation parameters, the same observer and a second independent observer repeated the analysis of 10 consecutive patients 1 week apart using the same two-dimensional echocardiographic loop and the same cardiac cycle. The Lin coefficient was calculated as an aggregate measure for agreement with a maximum range between −1 and +1. For continuous data, it represents an analog of the weighted κ coefficient determined for ordinal data.[67]

DISCLOSURES

None.

REFERENCES

1. de Jager DJ, Grootendorst DC, Jager KJ, van Dijk PC, Tomas LM, Ansell D, Collart F, Finne P, Heaf JG, De Meester J, Wetzels JF, Rosendaal FR, Dekker FW: Cardiovascular and noncardiovascular mortality among patients starting dialysis. *JAMA* 302: 1782–1789, 2009
2. Foley RN, Parfrey PS, Sarnak MJ: Clinical epidemiology of cardiovascular disease in chronic renal disease. *Am J Kidney Dis* 32[Suppl 3]: S112–S119, 1998
3. Foley RN, Parfrey PS, Sarnak MJ: Epidemiology of cardiovascular disease in chronic renal disease. *J Am Soc Nephrol* 9[Suppl]: S16–S23, 1998
4. Kalantar-Zadeh K, Block G, Humphreys MH, Kopple JD: Reverse epidemiology of cardiovascular risk factors in maintenance dialysis patients. *Kidney Int* 63: 793–808, 2003
5. Zoccali C: Left ventricular systolic dysfunction: A sudden killer in end-stage renal disease patients. *Hypertension* 56: 187–188, 2010
6. Green D, Roberts PR, New DI, Kalra PA: Sudden cardiac death in hemodialysis patients: An in-depth review. *Am J Kidney Dis* 57: 921–929, 2011
7. U.S. Renal Data System. Annual Data Report: Atlas of Chronic Kidney Disease and End-Stage Renal Disease in the US. Bethesda, MD, National Institutes of Health, Diabetes and Digestive and Kidney Disease, 2007.
8. Mizobuchi M, Nakamura H, Tokumoto M, Finch J, Morrissey J, Liapis H, Slatopolsky E: Myocardial effects of VDR activators in renal failure. *J Steroid Biochem Mol Biol* 121: 188–192, 2010
9. Zoccali C, Benedetto FA, Mallamaci F, Tripepi G, Giacone G, Cataliotti A, Seminara G, Stancanelli B, Malatino LS: Prognostic value of echocardiographic indicators of left ventricular systolic function in asymptomatic dialysis patients. *J Am Soc Nephrol* 15: 1029–1037, 2004
10. Becker M, Kramann R, Dohmen G, Luckhoff A, Autschbach R, Kelm M, Hoffmann R: Impact of left ventricular loading conditions on myocardial deformation parameters: Analysis of early and late changes of myocardial deformation parameters after aortic valve replacement. *J Am Soc Echocardiogr* 20: 681–689, 2007
11. Leitman M, Lysyansky P, Sidenko S, Shir V, Peleg E, Binenbaum M, Kaluski E, Krakover R, Vered Z: Two-dimensional strain-a novel software for real-time quantitative echocardiographic assessment of myocardial function. *J Am Soc Echocardiogr* 17: 1021–1029, 2004
12. Carasso S, Agmon Y, Roguin A, Keidar Z, Israel O, Hammerman H, Lessick J: Left ventricular function and functional recovery early and late after myocardial infarction: A prospective pilot study comparing two-dimensional strain, conventional echocardiography, and radionuclide myocardial perfusion imaging. *J Am Soc Echocardiogr* 26: 1235–1244, 2013
13. Shanks M, Thompson RB, Paterson ID, Putko B, Khan A, Chan A, Becher H, Oudit GY: Systolic and diastolic function assessment in fabry disease patients using speckle-tracking imaging and comparison with conventional echocardiographic measurements. *J Am Soc Echocardiogr* 26: 1407–1414, 2013
14. Fine NM, Crowson CS, Lin G, Oh JK, Villarraga HR, Gabriel SE: Evaluation of myocardial function in patients with rheumatoid arthritis using strain imaging by speckle-tracking echocardiography [published online ahead of print July 19, 2013]. *Ann Rheum Dis* doi: 10.1136/annrheumdis-2013-203314
15. Cusmà Piccione M, Zito C, Bagnato G, Oreto G, Di Bella G, Bagnato G, Carerj S: Role of 2D strain in the early identification of left ventricular dysfunction and in the risk stratification of systemic sclerosis patients. *Cardiovasc Ultrasound* 11: 6, 2013
16. Becker M, Lenzen A, Ocklenburg C, Stempel K, Kühl H, Neizel M, Katoh M, Kramann R, Wildberger J, Kelm M, Hoffmann R: Myocardial deformation imaging based on ultrasonic pixel tracking to identify reversible myocardial dysfunction. *J Am Coll Cardiol* 51: 1473–1481, 2008

17. Richand V, Lafitte S, Reant P, Serri K, Lafitte M, Brette S, Kerouani A, Chalabi H, Dos Santos P, Douard H, Roudaut R: An ultrasound speckle tracking (two-dimensional strain) analysis of myocardial deformation in professional soccer players compared with healthy subjects and hypertrophic cardiomyopathy. *Am J Cardiol* 100: 128–132, 2007
18. Ng AC, Delgado V, Bertini M, van der Meer RW, Rijzewijk LJ, Hooi Ewe S, Siebelink HM, Smit JW, Diamant M, Romijn JA, de Roos A, Leung DY, Lamb HJ, Bax JJ: Myocardial steatosis and biventricular strain and strain rate imaging in patients with type 2 diabetes mellitus. *Circulation* 122: 2538–2544, 2010
19. Krämer J, Niemann M, Liu D, Hu K, Machann W, Beer M, Wanner C, Ertl G, Weidemann F: Two-dimensional speckle tracking as a non-invasive tool for identification of myocardial fibrosis in Fabry disease. *Eur Heart J* 34: 1587–1596, 2013
20. Saito M, Okayama H, Yoshii T, Higashi H, Morioka H, Hiasa G, Sumimoto T, Inaba S, Nishimura K, Inoue K, Ogimoto A, Shigematsu Y, Hamada M, Higaki J: Clinical significance of global two-dimensional strain as a surrogate parameter of myocardial fibrosis and cardiac events in patients with hypertrophic cardiomyopathy. *Eur Heart J Cardiovasc Imaging* 13: 617–623, 2012
21. Popovic ZB, Kwon DH, Mishra M, Buakhamsri A, Greenberg NL, Thamilarasan M, Flamm SD, Thomas JD, Lever HM, Desai MY: Association between regional ventricular function and myocardial fibrosis in hypertrophic cardiomyopathy assessed by speckle tracking echocardiography and delayed hyperenhancement magnetic resonance imaging. *J Am Soc Echocardiogr* 21: 1299–1305, 2008
22. Popović ZB, Benejam C, Bian J, Mal N, Drinko J, Lee K, Forudi F, Reeg R, Greenberg NL, Thomas JD, Penn MS: Speckle-tracking echocardiography correctly identifies segmental left ventricular dysfunction induced by scarring in a rat model of myocardial infarction. *Am J Physiol Heart Circ Physiol* 292: H2809–H2816, 2007
23. Kansal MM, Panse PM, Abe H, Caracciolo G, Wilansky S, Tajik AJ, Khandheria BK, Sengupta PP: Relationship of contrast-enhanced magnetic resonance imaging-derived intramural scar distribution and speckle tracking echocardiography-derived left ventricular two-dimensional strains. *Eur Heart J Cardiovasc Imaging* 13: 152–158, 2012
24. Peng Y, Popovic ZB, Sopko N, Drinko J, Zhang Z, Thomas JD, Penn MS: Speckle tracking echocardiography in the assessment of mouse models of cardiac dysfunction. *Am J Physiol Heart Circ Physiol* 297: H811–H820, 2009
25. Gross ML, Ritz E: Hypertrophy and fibrosis in the cardiomyopathy of uremia—beyond coronary heart disease. *Semin Dial* 21: 308–318, 2008
26. Kennedy DJ, Vetteth S, Periyasamy SM, Kanj M, Fedorova L, Khouri S, Kahaleh MB, Xie Z, Malhotra D, Kolodkin NI, Lakatta EG, Fedorova OV, Bagrov AY, Shapiro JI: Central role for the cardiotonic steroid marinobufagenin in the pathogenesis of experimental uremic cardiomyopathy. *Hypertension* 47: 488–495, 2006
27. Flynn JT: Cardiovascular disease in children with chronic renal failure. *Growth Hormone IGF Res* 16[Suppl A]: S84–S90, 2006
28. London GM: Cardiovascular disease in chronic renal failure: Pathophysiologic aspects. *Semin Dial* 16: 85–94, 2003
29. Tian J, Shidyak A, Periyasamy SM, Haller S, Taleb M, El-Okdi N, Elkareh J, Gupta S, Gohara S, Fedorova OV, Cooper CJ, Xie Z, Malhotra D, Bagrov AY, Shapiro JI: Spironolactone attenuates experimental uremic cardiomyopathy by antagonizing marinobufagenin. *Hypertension* 54: 1313–1320, 2009
30. Haller ST, Drummond CA, Yan Y, Liu J, Tian J, Malhotra D, Shapiro JI: Passive immunization against marinobufagenin attenuates renal fibrosis and improves renal function in experimental renal disease [published online ahead of print September 6, 2013]. *Am J Hypertens* 10.1093/ajh/hpt169
31. Lekawanvijit S, Kompa AR, Manabe M, Wang BH, Langham RG, Nishijima F, Kelly DJ, Krum H: Chronic kidney disease-induced cardiac fibrosis is ameliorated by reducing circulating levels of a non-dialysable uremic toxin, indoxyl sulfate. *PLoS ONE* 7: e41281, 2012
32. Tyralla K, Adamczak M, Benz K, Campean V, Gross ML, Hilgers KF, Ritz E, Amann K: High-dose enalapril treatment reverses myocardial fibrosis in experimental uremic cardiomyopathy. *PLoS ONE* 6: e15287, 2011
33. Törnig J, Amann K, Ritz E, Nichols C, Zeier M, Mall G: Arteriolar wall thickening, capillary rarefaction and interstitial fibrosis in the heart of rats with renal failure: The effects of ramipril, nifedipine and moxonidine. *J Am Soc Nephrol* 7: 667–675, 1996
34. Vlahakos DV, Hahalis G, Vassilakos P, Marathias KP, Geroulanos S: Relationship between left ventricular hypertrophy and plasma renin activity in chronic hemodialysis patients. *J Am Soc Nephrol* 8: 1764–1770, 1997
35. Semple D, Smith K, Bhandari S, Seymour AM: Uremic cardiomyopathy and insulin resistance: A critical role for akt? *J Am Soc Nephrol* 22: 207–215, 2011
36. Semple DJ, Bhandari S, Seymour AM: Uremic cardiomyopathy is characterized by loss of the cardioprotective effects of insulin. *Am J Physiol Renal Physiol* 303: F1275–F1286, 2012
37. Amann K, Törnig J, Kugel B, Gross ML, Tyralla K, El-Shakmak A, Szabo A, Ritz E: Hyperphosphatemia aggravates cardiac fibrosis and microvascular disease in experimental uremia. *Kidney Int* 63: 1296–1301, 2003
38. Yamamoto KT, Robinson-Cohen C, de Oliveira MC, Kostina A, Nettleton JA, Ix JH, Nguyen H, Eng J, Lima JA, Siscovick DS, Weiss NS, Kestenbaum B: Dietary phosphorus is associated with greater left ventricular mass. *Kidney Int* 83: 707–714, 2013
39. Faul C, Amaral AP, Oskouei B, Hu MC, Sloan A, Isakova T, Gutiérrez OM, Aguillon-Prada R, Lincoln J, Hare JM, Mundel P, Morales A, Scialla J, Fischer M, Soliman EZ, Chen J, Go AS, Rosas SE, Nessel L, Townsend RR, Feldman HI, St John Sutton M, Ojo A, Gadegbeku C, Di Marco GS, Reuter S, Kentrup D, Tiemann K, Brand M, Hill JA, Moe OW, Kuro-O M, Kusek JW, Keane MG, Wolf M: FGF23 induces left ventricular hypertrophy. *J Clin Invest* 121: 4393–4408, 2011
40. Nguy L, Nilsson H, Lundgren J, Johansson ME, Teerlink T, Scheffer PG, Guron G: Vascular function in rats with adenine-induced chronic renal failure. *Am J Physiol Regul Integr Comp Physiol* 302: R1426–R1435, 2012
41. Katsumata K, Kusano K, Hirata M, Tsunemi K, Nagano N, Burke SK, Fukushima N: Sevelamer hydrochloride prevents ectopic calcification and renal osteodystrophy in chronic renal failure rats. *Kidney Int* 64: 441–450, 2003
42. Kramann R, DiRocco DP, Humphreys BD: Understanding the origin, activation and regulation of matrix-producing myofibroblasts for treatment of fibrotic disease. *J Pathol* 231: 273–289, 2013
43. Martin FL, McKie PM, Cataliotti A, Sangaralingham SJ, Korinek J, Huntley BK, Oehler EA, Harders GE, Ichiki T, Mangiafico S, Nath KA, Redfield MM, Chen HH, Burnett JC Jr: Experimental mild renal insufficiency mediates early cardiac apoptosis, fibrosis, and diastolic dysfunction: A kidney-heart connection. *Am J Physiol Regul Integr Comp Physiol* 302: R292–R299, 2012
44. Pandya K, Kim HS, Smithies O: Fibrosis, not cell size, delineates beta-myosin heavy chain reexpression during cardiac hypertrophy and normal aging in vivo. *Proc Natl Acad Sci U S A* 103: 16864–16869, 2006
45. Chaykovska L, von Websky K, Rahnenführer J, Alter M, Heiden S, Fuchs H, Runge F, Klein T, Hocher B: Effects of DPP-4 inhibitors on the heart in a rat model of uremic cardiomyopathy. *PLoS ONE* 6: e27861, 2011
46. Migrino RQ, Aggarwal D, Konorev E, Brahmbhatt T, Bright M, Kalyanaraman B: Early detection of doxorubicin cardiomyopathy using two-dimensional strain echocardiography. *Ultrasound Med Biol* 34: 208–214, 2008
47. Ersbøll M, Andersen MJ, Valeur N, Mogensen UM, Fahkri Y, Thune JJ, Møller JE, Hassager C, Søgaard P, Køber L: Early diastolic strain rate in relation to systolic and diastolic function and prognosis in acute myocardial infarction: a two-dimensional speckle-tracking study [published online ahead of print May 26, 2013]. *Eur Heart J* doi: 10.1093/eurheartj/eht179

48. Kimura K, Takenaka K, Ebihara A, Okano T, Uno K, Fukuda N, Ando J, Fujita H, Morita H, Yatomi Y, Nagai R: Speckle tracking global strain rate E/E' predicts LV filling pressure more accurately than traditional tissue Doppler E/E'. *Echocardiography* 29: 404–410, 2012
49. Azevedo CF, Amado LC, Kraitchman DL, Gerber BL, Osman NF, Rochitte CE, Edvardsen T, Lima JA: Persistent diastolic dysfunction despite complete systolic functional recovery after reperfused acute myocardial infarction demonstrated by tagged magnetic resonance imaging. *Eur Heart J* 25: 1419–1427, 2004
50. Schelbert EB, Hsu LY, Anderson SA, Mohanty BD, Karim SM, Kellman P, Aletras AH, Arai AE: Late gadolinium-enhancement cardiac magnetic resonance identifies postinfarction myocardial fibrosis and the border zone at the near cellular level in ex vivo rat heart. *Circ Cardiovasc Imaging* 3: 743–752, 2010
51. Reiter T, Ritter O, Prince MR, Nordbeck P, Wanner C, Nagel E, Bauer WR: Minimizing risk of nephrogenic systemic fibrosis in cardiovascular magnetic resonance. *J Cardiovasc Magn Reson* 14: 31, 2012
52. Cho GY, Marwick TH, Kim HS, Kim MK, Hong KS, Oh DJ: Global 2-dimensional strain as a new prognosticator in patients with heart failure. *J Am Coll Cardiol* 54: 618–624, 2009
53. Liu YW, Su CT, Huang YY, Yang CS, Huang JW, Yang MT, Chen JH, Tsai WC: Left ventricular systolic strain in chronic kidney disease and hemodialysis patients. *Am J Nephrol* 33: 84–90, 2011
54. Gulel O, Soylu K, Yuksel S, Karaoglanoglu M, Cengiz K, Dilek M, Hamiseyev C, Kale A, Arik N: Evidence of left ventricular systolic and diastolic dysfunction by color tissue Doppler imaging despite normal ejection fraction in patients on chronic hemodialysis program. *Echocardiography* 25: 569–574, 2008
55. Yan P, Li H, Hao C, Shi H, Gu Y, Huang G, Chen J: 2D-speckle tracking echocardiography contributes to early identification of impaired left ventricular myocardial function in patients with chronic kidney disease. *Nephron Clin Pract* 118: c232–c240, 2011
56. Edwards NC, Hirth A, Ferro CJ, Townend JN, Steeds RP: Subclinical abnormalities of left ventricular myocardial deformation in early-stage chronic kidney disease: The precursor of uremic cardiomyopathy? *J Am Soc Echocardiogr* 21: 1293–1298, 2008
57. Rakhit DJ, Zhang XH, Leano R, Armstrong KA, Isbel NM, Marwick TH: Prognostic role of subclinical left ventricular abnormalities and impact of transplantation in chronic kidney disease. *Am Heart J* 153: 656–664, 2007
58. Liu YW, Su CT, Sung JM, Wang SP, Su YR, Yang CS, Tsai LM, Chen JH, Tsai WC: Association of left ventricular longitudinal strain with mortality among stable hemodialysis patients with preserved left ventricular ejection fraction. *Clin J Am Soc Nephrol* 8: 1564–1574, 2013
59. Stoylen A, Heimdal A, Bjornstad K, Wiseth R, Vik-Mo H, Torp H, Angelsen B, Skjaerpe T: Strain rate imaging by ultrasonography in the diagnosis of coronary artery disease. *J Am Soc Echocardiogr* 13: 1053–1064, 2000
60. Saravanan P, Davidson NC: Risk assessment for sudden cardiac death in dialysis patients. *Circ Arrhythm Electrophysiol* 3: 553–559, 2010
61. Watson LE, Sheth M, Denyer RF, Dostal DE: Baseline echocardiographic values for adult male rats. *J Am Soc Echocardiogr* 17: 161–167, 2004
62. Price PA, Roublick AM, Williamson MK: Artery calcification in uremic rats is increased by a low protein diet and prevented by treatment with ibandronate. *Kidney Int* 70: 1577–1583, 2006
63. Slama M, Susic D, Varagic J, Ahn J, Frohlich ED: Echocardiographic measurement of cardiac output in rats. *Am J Physiol Heart Circ Physiol* 284: H691–H697, 2003
64. Pieper GM, Shah A, Harmann L, Cooley BC, Ionova IA, Migrino RQ: Speckle-tracking 2-dimensional strain echocardiography: A new noninvasive imaging tool to evaluate acute rejection in cardiac transplantation. *J Heart Lung Transplant* 29: 1039–1046, 2010
65. Kramann R, Couson SK, Neuss S, Kunter U, Bovi M, Bornemann J, Knüchel R, Jahnen-Dechent W, Floege J, Schneider RK: Exposure to uremic serum induces a procalcific phenotype in human mesenchymal stem cells. *Arterioscler Thromb Vasc Biol* 31: e45–e54, 2011
66. Becker M, Kramann R, Franke A, Breithardt OA, Heussen N, Knackstedt C, Stellbrink C, Schauerte P, Kelm M, Hoffmann R: Impact of left ventricular lead position in cardiac resynchronization therapy on left ventricular remodelling. A circumferential strain analysis based on 2D echocardiography. *Eur Heart J* 28: 1211–1220, 2007
67. Lin LI: A concordance correlation coefficient to evaluate reproducibility. *Biometrics* 45: 255–268, 1989

This article contains supplemental material online at http://jasn.asnjournals.org/lookup/suppl/doi:10.1681/ASN.2013070734/-/DCSupplemental.